CHEMISTRY
A EUROPEAN JOURNAL

DOI: 10.1002/chem.200701467

Efficient CO_2 Capturer Derived from As-Synthesized MCM-41 Modified with Amine

Ming Bo Yue,[a] Lin Bing Sun,[a] Yi Cao,[a] Ying Wang,*[b, c] Zhu Ji Wang,[b] and Jian Hua Zhu*[a]

Abstract: A new strategy to synthesize a highly efficient CO_2 capturer by incorporating tetraethylenepentamine (TEPA) into as-synthesized MCM-41 (AM) is reported. The amine guest can be distributed in the micelle of the support, forming a web within the mesopore to trap CO_2 molecules and resulting in a high adsorption capacity for CO_2 up to 237 mg g^{-1}. Four samples of the as-synthesized MCM-41 with a different amount or type of surfactant are employed as supports to investigate the influence of micelles on the CO_2 adsorption, and the spokelike structure of the micelle in the channel of the support is proven to be essential to the distribution of guest amine. Among these supports, the AM sample is the most competitive due to the advantages of energy and time saving in preparation of the support along with the resulting higher CO_2 adsorption capacity. At the optimal loading of 50 wt % TEPA, the AM-50 sample exhibits a high adsorption capacity of 183 mg g^{-1} in the sixth adsorption cycle at 5 % CO_2 concentration.

Keywords: adsorption · amines · carbon dioxide · mesoporous materials · micelles

Introduction

Carbon dioxide is one of the greenhouse gases that causes global warming and its concentration has increased by 90 ppm (480 billion tons) in about 200 years since 1800. Rather, it has increased recently by about 1.5 ppm (8 billion tons) per year.[1,2] Therefore, how to control carbon dioxide emission and, more importantly, how to use this greenhouse gas as a carbon resource to produce fine chemicals and materials has become an urgent global issue.[2,3] However, one of the barriers for CO_2 sequestration or utilization is the high cost of CO_2 capture, separation, and purification;[3] hence, it is necessary to prepare novel efficient adsorbents to capture CO_2 in the environment at low cost. To overcome the drawbacks of amine aqueous solutions, in which the concentration of amine in the aqueous phase is limited due to viscosity and foaming issues,[4] solid adsorbents have earned much attention. Apart from the efforts in preparing solid adsorbents, such as zeolites and hydrotalcite,[5,6] introducing amines into porous supports like silica gel or carbon is a feasible method.[7,8]

In general, there are two ways to introduce amine into the solid supports. One is to graft amine groups on the support surface and the other is to load amines through impregnation. Three methods can be used for the grafting of amine: postsynthesis grafting,[9,10] direct synthesis by co-condensation,[11] and anionic template synthesis with the help of the interaction between the cation head in monoaminosilane and anionic surfactants.[12] For the removal of CO_2, grafting amine onto silica through postsynthesis has been widely used. Various kinds of silica, such as silica gel,[7] MCM-41,[13] MCM-48,[14] and SBA-15,[15–17] were employed as the support. In addition, different amines were grafted onto the surface of the porous support to investigate the impact of amine types on the CO_2 adsorption capacity of the resulting composites. For example, Hiyoshi introduced three kinds of amine into SBA-15 to study the influence of amine type on

[a] Dr. M. B. Yue, L. B. Sun, Dr. Y. Cao, Prof. Dr. J. H. Zhu
Key Laboratory of Mesoscopic Chemistry
School of Chemistry & Chemical Engineering
Nanjing University
Nanjing 210093 (China)
Fax: (+86) 25-8331-7761
E-mail: jhzhu@netra.nju.edu.cn

[b] Prof. Dr. Y. Wang, Z. J. Wang
Department of Chemistry
School of Chemistry & Chemical Engineering
Nanjing University
Nanjing 210093 (China)
E-mail: wangy@netra.nju.edu.cn

[c] Prof. Dr. Y. Wang
Ecomaterials and Renewable Energy Research Center (ERERC)
Nanjing University
Nanjing 210093 (China)

the CO_2 adsorption performance,[15] and found an increased adsorption capacity of 0.52, 0.87, and 1.10 mmol g^{-1} in the monoamino-, diamino-, and triamino-grafted SBA-15 samples, respectively. It is very likely that the resulting CO_2 adsorption capacity of the composite is proportional to the number of amine groups grafted in the porous adsorbent. Usually, this type of adsorbent, which is obtained by grafting of amine-containing alkoxysilanes onto the support surface, has a relatively higher thermal stability and thus it can be applied at high temperature. Furthermore, these amine groups can be well distributed on the surface of the support to exhibit a high efficiency for capture of CO_2. However, a problem with grafting amine onto solid supports is the limited quantity of amine retained on the support due to the limited density of surface silanol groups, which leads to a relatively low CO_2 adsorptive capability of the resulting composite. For instance, the CO_2 adsorption capacity observed on the monoamine-grafted MCM-48 was only 1.14 mmol g^{-1}.[14]

Unlike the grafting method in which the number of amine guests introduced on the porous host is restricted, a larger amount of amine can be loaded on the support by an impregnation procedure. The final adsorption capacity for CO_2 of adsorbents fabricated through impregnation depends chiefly on the amount of amine loaded and the distribution of the amine groups. For example, amine–MCM-41 composites with various loading amounts of polyethyleneimine (PEI) exhibited different adsorptive capacities from 7.7 to 133 mg g^{-1} at 348 K,[18,19] mirroring the fact that the amount of amine loaded dominates the capacity for CO_2 adsorption. To make a new support with larger pore volume to accommodate more amine groups, Sayari and co-workers used pore-expanded mesoporous MCM-41 to host a greater quantity of diethanolamine, which resulted in a CO_2 adsorption capacity of 2.65 mmol g^{-1} (116.6 mg g^{-1}).[20] As more amines can be loaded on the support through impregnation, the resulting composite has a larger CO_2 adsorption capacity than the analogue obtained by grafting.[13,21] Nonetheless, the distribution of the amine groups in the composite also plays a significant role in the adsorption of CO_2; the high dispersion enables the amine to exhibit high accessibility, hence more CO_2 can be captured by the composite in adsorption procedures. The distribution of amine introduced into the porous support by impregnation is inferior to that obtained by grafting, and the amine guest often conglomerates in the host, which results in a relatively low efficiency of amine in the adsorption of CO_2.

To load a large amount of amine on a porous material, such as that with the impregnation procedure, and to keep it well dispersed and distributed, similar to that by the grafting method, we tried to utilize as-synthesized SBA-15 as the support to load the amine through impregnation.[21] In the as-synthesized SBA-15, the propylene oxide blocks of P123 are distributed within the pores of SBA-15 like branches, while the ethylene oxide blocks are rooted within the framework.[21,22] The amine guest can be dispersed in the micelle with a good accessibility towards CO_2; therefore, the obtained composites have a high CO_2 adsorption capacity of 173 mg g^{-1}.[21] To further pursue the higher efficiency in capturing CO_2, we chose the as-synthesized MCM-41 as a candidate, because MCM-41 possesses a narrower channel than SBA-15 so that each gram of template-free MCM-41 can contain more channels than SBA-15, which should be beneficial for the dispersion of the loaded amine.

As-synthesized MCM-41, prepared with the direction of cetyltrimethylammonium bromide (CTAB, ionic surfactant), is different from as-synthesized SBA-15 in the distribution of surfactant micelles occluded inside the pores. In general, ionic surfactants have a stronger interaction with the silica wall in comparison to the amphiphilic block copolymers in SBA-15. As a result of this stronger interaction, CTAB disperses in the channel of MCM-41 like the spokes in a wheel, with the cation head rooted on the silica wall. In addition, less space remains in the as-synthesized MCM-41 between the silica wall and the template than that in as-synthesized SBA-15. On the other hand, the hydrophobicity of CTAB carbon tails can enable the additives, such as amine or benzene, to be incorporated easily into the micelle.[23–25] With this function, surfactant-containing MCM-41 has been tested in the adsorption of organics from solution or a gas flow.[26,27] Some questions arise from these known facts. Can tetraethylenepentamine (TEPA) be incorporated into the micelle of as-synthesized MCM-41, too? What is the influence of the micelle on the TEPA distribution and the succeeding CO_2 adsorption? Here, we try to answer these queries by utilizing the micelles in the as-synthesized MCM-41 to disperse amine for the first time, directly introducing TEPA into the MCM-41 to coat the micelles and to develop an efficient CO_2 capturer. In addition, various kinds of MCM-41 sample with different amounts or type of surfactant remaining within the channel have been used as supports for a deeper understanding of amine distribution in the surfactant micelles and, more importantly, for investigating the influence of micelles on the final CO_2 capture capability of the obtained composites.

Abstract in Chinese:

本文以MCM-41原粉（AM）为载体，通过负载四乙烯五胺制备了新型的二氧化碳吸附材料。利用胺束在孔道里的丝状分布以及它们和硅壁之间的亚纳米间隙，进行网状涂布和分散有机胺，形成具有高拦截效率的吸附材料，吸附量达到237 mg g^{-1}。以四种具有不同表面活性剂类型和含量的介孔MCM-41作为载体，考察了胺束对二氧化碳吸附的影响。MCM-41原粉（AM）孔道中的轮辐状胺束结构有利于客体分子的涂布，其四乙烯五胺的最佳分布量为50 wt%，所得到的吸附剂在5% CO_2中经六次循环吸附后其吸附量仍可达到183 mg g^{-1}。因此，以含有模板剂的介孔氧化硅材料为载体、负载有机胺制备二氧化碳吸附剂，不但提高了材料的二氧化碳吸附量，而且节省了焙烧除去模板剂的能源，在降低了成本的同时还减少了对于环境的污染。

Results and Discussion

Textural properties of the amine–MCM-41 composites: Figure 1 and Table 1 present the nitrogen adsorption data of

as-synthesized MCM-41 and the TEPA-modified analogues. Three porous supports of MCM-41 occluded with template are employed, termed AM, EM, and PM. All CTAB templates are reserved in the AM sample, while part of the template in the EM sample is extracted with ethanol. For the PM sample, its synthesis used trimethylbenzene (TMB) as swelling agent and the obtained sample is extracted to remove TMB but the CTAB remains. As seen from the N_2 adsorption isotherms (Figure 1), the three samples occluded with template do not exhibit the typical condensation steps of MCM-41 at the relative pressure p/p_0 of 0.3. There is no accessible primary mesopore formed during the water-washing process because of the strong electrostatic forces between the CTAB template and silica wall, which differs from that of SBA-15 occluded with template where 63% of the total pore volume was free after water washing.[21]

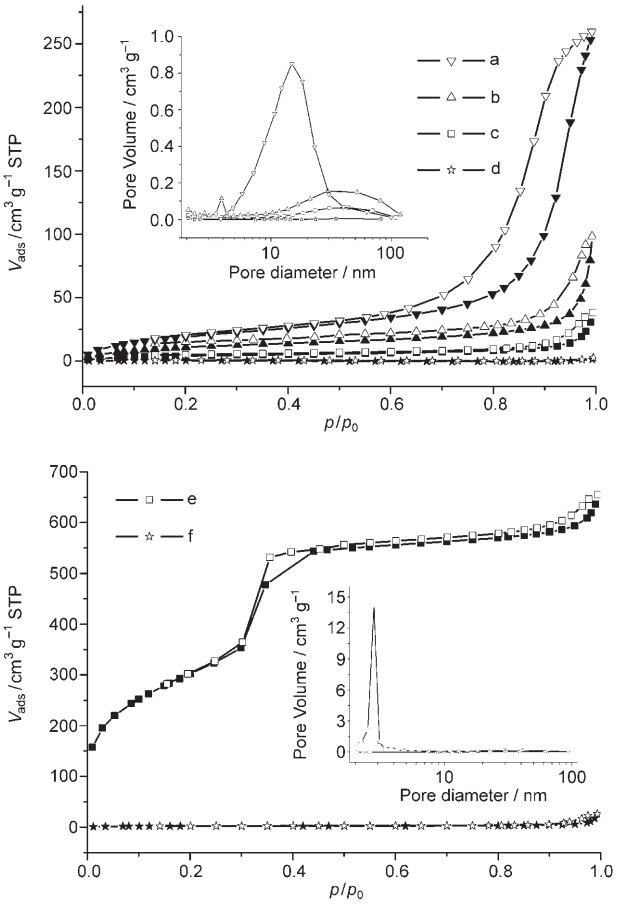

Figure 1. Nitrogen adsorption–desorption isotherms of a) PM, b) EM, c) AM, d) EM-50, e) CM, and f) CM-50 samples.

Table 1. Textural properties of supports and the amine-modified MCM-41 composites.

Sample	S_{BET}[a] [m^{2}g^{-1}]	V_p[b] [cm^{3}g^{-1}]
CM	1342	1.01
AM	16	0.03
EM	45	0.08
PM	76	0.36
EM-50	1.5	0.002
CM-50	7.8	0.01

[a] Brunauer–Emmett–Teller (BET) surface area. [b] Pore volume.

Occupation of the channel in the mesoporous silica by the CTAB template results in the absence of MCM-41 condensation steps in the N_2 adsorption isotherms. Nonetheless, the AM sample gives a hysteresis loop at relative pressure $p/p_0 > 0.8$ and exhibits a small surface area (16 m^{2}g^{-1}) and pore volume (0.03 cm^{3}g^{-1}). Sample EM also presents a hysteresis loop at relative pressure $p/p_0 > 0.8$, slightly larger than that of AM, owing to the partial removal of the CTAB template. Likewise, the EM sample has a relatively larger surface area (45 m^{2}g^{-1}) and pore volume (0.08 cm^{3}g^{-1}). As a template-free sample, CM exhibits the typical N_2 adsorption isotherms of MCM-41, and its surface area and pore volume are enlarged to 1342 m^{2}g^{-1} and 1.01 cm^{3}g^{-1}, respectively. With the same amounts of template occluded in the mesopore as that in the AM sample, the PM sample does not show the typical MCM-41 condensation steps in the N_2 adsorption isotherms either. However, it exhibits a larger hysteresis loop than AM in the range of relative pressure $p/p_0 =$ 0.6–1.0, due to the removal of TMB which congregates in the core of the CTAB micelle. The surface area of PM enlarges slightly to 76 m^{2}g^{-1} while its pore volume achieves 0.36 cm^{3}g^{-1}, both larger than those of the AM sample. After loading 50 wt% TEPA, the N_2 adsorption isotherms of samples CM and EM become linear (curves d and f in Figure 1); meanwhile, both the surface area and the pore volume decrease distinctly. For instance, the pore volume of the CM sample is lowered from 1.01 (CM) to 0.01 cm^{3}g^{-1}(CM-50).

These phenomena demonstrate the occupation of the pore in the support by the amine guest. In addition, as is evident from the X-ray diffraction (XRD) patterns (samples e and f in Figure 2), the reflection intensities of the CM-50 sample diminish, which coincides with the report on MCM-41-loaded PEI[18,19] and SBA-15 modified with TEPA.[21] It is known that the reflection intensities are related to the degree of pore filling and the scattering contrast between the pore walls and the inside of the pores.[28–30] Hence, the loss of scattering intensity indicates a loss of scattering contrast, which is caused by the incorporation of TEPA into the channels of the support.

As illustrated in Figure 1 and Table 1, there is no mesopore in the AM support, and thus the space available for the encapsulation of TEPA is very limited. However, the

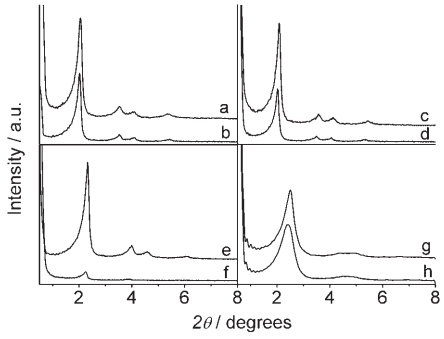

Figure 2. XRD patterns of MCM-41 samples. a) AM, b) AM-50, c) EM, d) EM-50, e) CM, f) CM-50, g) DM, and h) DM-50.

composite derived from AM is different from the others prepared through impregnating TEPA on nonporous supports, such as quartz. As reported in the literature,[20] when porous materials were used as supports, the texture of the resulting materials changed from a free-flowing powder to an agglomerated powder when the amine loading exceeded the pore saturation and the additional guests were deposited on the external surface of the adsorbent. The amine–quartz composite became viscous or gel-like and conglomerated together, even when only 10 wt% TEPA was loaded.

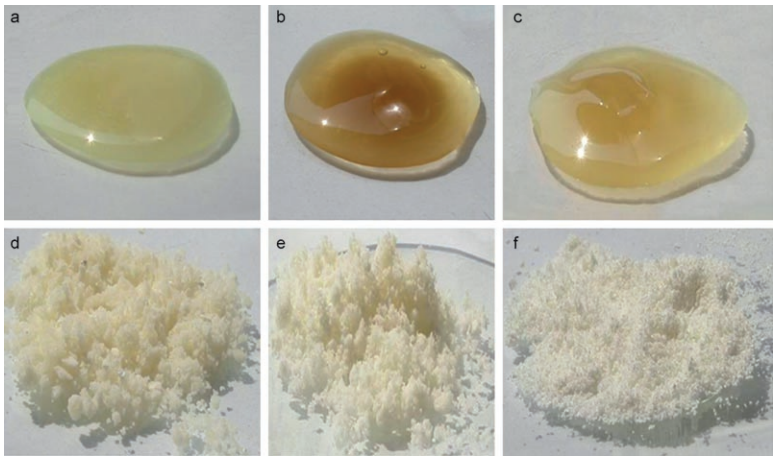

Figure 3. Morphology of the amine composites prepared based on a) quartz, b) KA zeolite, c) NaA zeolite, d) NaY zeolite, e) AM, and f) CM loaded with 50 wt% TEPA.

Figure 3 depicts the morphology of various amine-containing composites consisting of 50 wt% TEPA. Due to the lack of pores to accommodate amine molecules and the small surface area, the quartz sample mixed with TEPA gave a gel-like composite (sample a in Figure 3). Despite the larger surface area than that of quartz, NaA and KA zeolites also form gels with the amine, the reason being their small pore opening (0.4 nm for NaA and 0.3 nm for KA zeolites). TEPA hardly enters the pores of NaA and KA, and therefore it has to be loaded on the external surface, so the texture of these three samples prepared from quartz, NaA, and KA is similar. Contrarily, NaY zeolite has an aperture of 0.74 nm, which allows the amine to enter freely, and therefore the texture of the resulting amine–zeolite composite is a powder instead of a gel (sample d in Figure 3). When the mesoporous material CM, template-free MCM-41, was utilized as the support, the texture of the resulting composite was a powder (sample f in Figure 3), similar to that of amine–NaY zeolite. This is expected because the larger pore diameter and pore volume of MCM-41 enable more guests to be accommodated in the channel much more easily. Sample e in Figure 3 is the composite derived from AM, the as-synthesized MCM-41, and it is clearly a well-separated powder even when 50 wt% TEPA is loaded. Based on these comparisons, it is safe to conclude that the TEPA guest ought to be mainly located inside the palisade of the as-synthesized MCM-41 host; otherwise, the resulting composite should have a gel-like morphology, although the available data do not allow a detailed discussion of the amine distribution.

In the channel of the AM sample, the charged head group of the micelle interacts with the siliceous wall through electrostatic interaction and the hydrophobic carbon chain is well distributed in the pore of MCM-41. Even so, organic molecules can still be adsorbed by a process often termed "adsolubilization".[26] There are two ways of solving the guest molecule into the surfactant micelles.[31,32] One is solubilization in the palisade layer of the micelle, from which the guest molecules penetrate into the surfactant palisade layer and have little influence on the micellar diameter. The other is dissolution in the core of the micelle, in which the guest molecules conglomerate and expand the volume of the micelles. Polar molecules, such as alkylamine and alkyl alcohol, dissolve in the palisade of the micelle, whereas nonpolar molecules, such as TMB, dissolve in the core of the micelle as a swelling agent to enlarge the pores of mesoporous silica. As a polar molecule, TEPA is well dissolved in ethanol. However, in the process of solvent evaporation, TEPA transfers from solution to the palisade of the CTAB micelle and distributes in the as-synthesized MCM-41, but does not enlarge the micelle.[33,34] The XRD patterns of the TEPA-modified as-synthesized MCM-41 sample are close to that of the host itself, except for the decrease in reflection intensities (Figure 2), which indicates the insertion of TEPA inside the pore of the host.

Figure 4 depicts the thermogravimetry (TG) curves of AM and AM-50 samples; the former shows three weight losses, which is in good agreement with the literature.[32] Removal of physically adsorbed water and CO_2 is observed below 150 °C; the weight loss between 150 and 250 °C is assigned to Hofmann elimination of trimethylamine in the CTAB template, which leads to a hydrocarbon chain remaining in the porous support. The third weight loss in the range of 250–350 °C originates from a carbon-chain fragmentation accompanied by oxidation processes. After encapsulation of TEPA (50 wt%) in the AM sample, the resulting composite exhibits three weight losses of 15, 18, and 40 wt%, respectively. Physically adsorbed water and CO_2 are removed from the composite below 140 °C, giving a weight loss of 15 wt%; decomposition of the template via Hofmann degradation occurs between 140 and 200 °C, as the base (TEPA) facilitates the elimination of the trimethylamine head group.[35] The third weight loss begins around 200 °C and reaches a maximum near 400 °C; this loss of

40 wt% results from a successive carbon-chain (residue of CTAB and TEPA) fragmentation or decomposition with oxidation reactions. FTIR measurements further confirm the incorporation of the TEPA guest in the AM-50 sample (Figure 5); the appearance of additional peaks around 1582 and 1302 cm^{-1} indicates the presence of amine groups in the AM-50 sample.

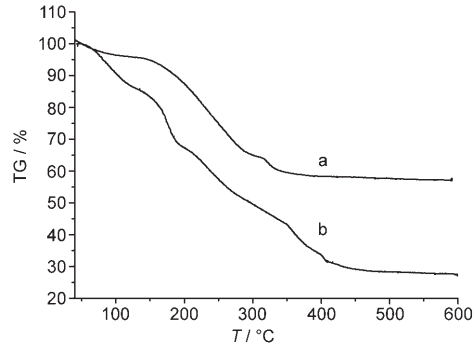

Figure 4. TG curves of a) AM and b) AM-50 heated at a rate of 10 °C min^{-1} from 35 to 600 °C.

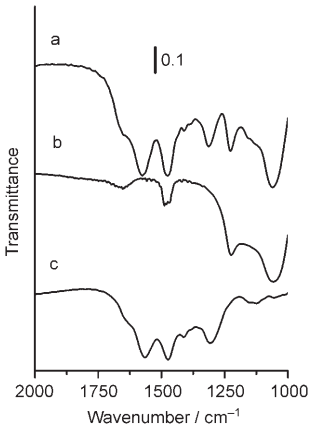

Figure 5. IR spectra of a) AM-50, b) AM, and c) TEPA itself.

In addition, the elemental analysis results for AM (Table 2) before and after modification with TEPA provide further proof of the incorporation of TEPA in the MCM-41 occluded with template. The C/N molar ratio of the AM sample, calculated from the data for elemental analysis, is 19.1, in agreement with the value for CTAB (19). After modification with TEPA, the C/N molar ratio of the AM-50 sample significantly decreases to 2.92, due to the incorporation of TEPA whose C/N ratio is very low (1.6). Similarly, the C/N molar ratio of the DM sample, the as-synthesized MCM-41 sample occluded with the template dodecyltrimethylammonium bromide (DTAB), decreases from 14.87 to 2.43 after loading 40 wt% TEPA on the support (DM-40). The decrease of the C/N molar ratio of the sample after modification with TEPA means the introduction of amines into the composite. In addition, the molar ratio of TEPA/template can be calculated from the elemental N weight percentage variation before and after modification by TEPA, and is shown in Table 2.

Table 2. Elemental analysis and the calculated TEPA/template molar ratio of the amine-modified MCM-41 composites.

Support	AM	AM-50	DM	DM-40
C [wt%]	34.75	44.93	32.63	38.26
H [wt%]	7.61	10.97	6.07	8.13
N [wt%]	2.12	17.93	2.43	14.87
TEPA/template[a]	–	3.18	–	1.84

[a] The molar ratio of TEPA/template was calculated from the elemental N weight-percentage variation before and after modification by TEPA. In samples AM-50 and DM-40, the molar ratios were calculated as TEPA/CTAB = $[(17.93-2.12\times0.5)/5]/(2.12\times0.5)=3.18$ and TEPA/DTAB = $[(14.87-2.43\times0.6)/5]/(2.43\times0.6)=1.84$, respectively.

Adsorption of CO_2 by the amine–MCM-41 composites: Figure 6 displays the CO_2 temperature-programmed desorption (TPD) profile of AM-*n* samples that are loaded with different amounts of amine. Only a small amount of CO_2 is desorbed from the AM sample, which means that the CO_2 adsorption capacity of AM itself is very low. As the amount of TEPA loaded increases, the CO_2 TPD peak grows in the profile and the peak maximum shifts to a higher temperature, indicating the larger capacity and the stronger adsorption of CO_2 on the amine-modified composites. By the way, most of the trapped CO_2 can be desorbed from the sample at 100 °C, thus facilitating the regeneration and recycle capability of the adsorbents.

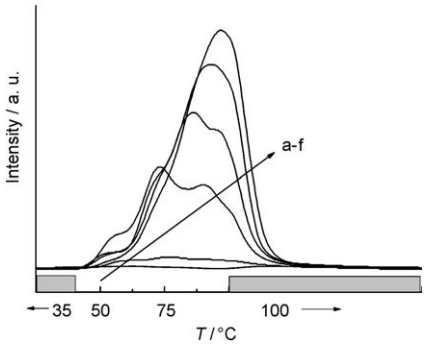

Figure 6. CO_2 TPD profile of AM-*n* samples performed at a rate of 2.5 °C min^{-1} from 35 to 100 °C and held at 100 °C for 0.5 h. The weight percentage of TEPA in the composite was a) 0, b) 10, c) 30, d) 40, e) 50, and f) 60 wt%.

Figure 7 demonstrates the TG–differential scanning calorimetry (DSC) curves of the AM-50 sample for CO_2 adsorbed at 75 °C. The weight of the AM-50 composite dramatically increases to 110% of the original value after exposure to CO_2 for 1.5 min, while the DSC curve shows an exothermic peak (1.82 mW mg^{-1}) at the same time. After another 5 min of exposure to CO_2, the weight of the sample rises to 118% in comparison with its original data. When the adsorption time is prolonged to 140 min, the weight of the

sample slowly increases to 119.8% of the original value. These results mean that this composite can reach half of its adsorption capacity within 1.5 min and the corresponding adsorption rate is 67 $mg\,g^{-1}\,min^{-1}$. Nevertheless, the adsorption rate of AM-50 declines to 16 $mg\,g^{-1}\,min^{-1}$ in the subsequent 5 min and the remaining 40% of the adsorption by this composite is completed in this period. In particular, more than 130 min is needed to finish the residual 10% adsorption and the corresponding adsorption rate is only 0.21 $mg\,g^{-1}\,min^{-1}$. It appears that the adsorption of CO_2 in the AM-50 sample is a kinetically (diffusion) controlled process, similar to that observed in other amine-modified mesoporous silica materials.[18,19,21] The affinity sites on the surface of TEPA particles in the mesopores react with CO_2 more readily than those within the TEPA particles because of diffusion limitations.

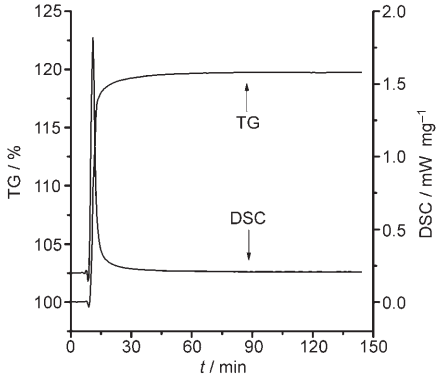

Figure 7. TG and DSC curves of the AM-50 sample for CO_2 adsorption at 75°C.

Figure 8 exhibits the TG-DSC and mass spectrometry (MS) curves of the CO_2 desorption in the AM-50 sample from 35 to 100°C. Only 2.5% of the CO_2 adsorbed is desorbed in the range of 35–60°C, which coincides with the CO_2 TPD curve of AM-50. As represented by curve e in Figure 6, the profile of CO_2 TPD on the AM-50 sample increases slowly before 60°C, indicating the small quantity of CO_2 to be desorbed. However, this curve rises rapidly once the temperature exceeds 60°C, and hence 26.5% of the CO_2 captured by the adsorbent escapes from the composite in the range of 60–80°C, as calculated from the TG data. Upon heating the sample from 80 to 100°C, about 53% of the adsorbate desorbs from the composite and the residual 18% of adsorbed CO_2 is released by holding the sample at 100°C for about 0.5 h, as confirmed by MS analysis.

Influence of TEPA loading on the CO_2 adsorption by MCM-41 composite: Figure 9 depicts the influence of TEPA on the CO_2 adsorption capacity of MCM-41 composites. The porous support alone, either AM or CM, has a weak CO_2 adsorption capacity around 2 $mg\,g^{-1}$ (Figure 9A). Loading TEPA on the as-synthesized MCM-41 (AM) increases the adsorption capacity of the composite substantially. For example, the sample exhibits an adsorption capacity of 24, 120,

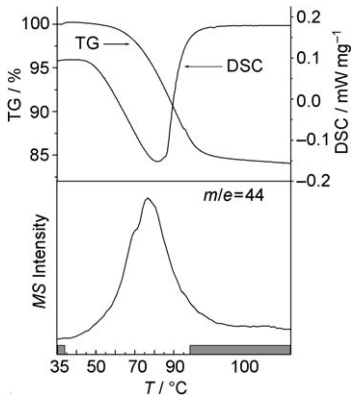

Figure 8. TG-DSC and MS curves of CO_2 desorption for the AM-50 sample heated at a rate of 2.5°C min^{-1} from 35 to 100°C and then held at 100°C.

167, 211, and 221 $mg\,g^{-1}$ when it is modified with TEPA of 10, 30, 40, 50, and 60 wt%, respectively. After loading with TEPA to 40 wt%, the AM-40 sample possesses a CO_2 adsorption capacity (167 $mg\,g^{-1}$) higher than that of pure TEPA (151 $mg\,g^{-1}$). On the contrary, the CM-*n* sample with TEPA loadings of 10, 30, 40, 50, and 60 wt% shows a CO_2 adsorption capacity of 8.8, 62, 102, 144, and 176 $mg\,g^{-1}$, respectively, which is much lower than the data for the corresponding AM-*n* analogues. For example, the CM-50 sample has an adsorption capacity of 144 $mg\,g^{-1}$, obviously lower than that of AM-50 (211 $mg\,g^{-1}$). Nonetheless, both series of amine-containing composites, AM-*n* and CM-*n*, perform with an enhanced adsorption activity towards CO_2 in comparison with the pure TEPA itself. If the support and the amine were simply mixed and separately exerted their functions in the adsorption of CO_2, the corresponding calculated adsorption capacities of the CM-50 and AM-50 samples should be 76.5 $mg\,g^{-1}$ $(151\times0.5+2\times0.5)$ and 76.7 $mg\,g^{-1}$ $(151\times0.5+2.4\times0.5)$, respectively, which are clearly lower than the data detected by experiment (144 and 211 $mg\,g^{-1}$). Thus, there should be a synergy between the guest TEPA and the porous supports in the adsorption of CO_2.

However, a new question arises from the different CO_2 adsorption capacities of CM-*n* and AM-*n* samples loaded with the same amount of TEPA: what causes such diversity? The reason, as has been previously reported,[18,19,21] is the distribution of amine on the porous support, which is crucial to the adsorption capacity. The good dispersion and distribution of the guest enable most of the loaded amine, if not all, to be accessible towards the CO_2 adsorbate and thus distinctly enhance the final adsorption ability of the resulting composite. The uniform channels of MCM-41 can provide a large surface area for the accommodation of amine. Therefore, a relatively homogeneous distribution of TEPA is achieved, and thus more CO_2 affinity sites can be exposed to the adsorbate, similar to that observed in the PEI-modified MCM-41 and TEPA-modified SBA-15 samples.[18,19,21] However, the template micelles occluded inside the channel of AM supply another delicate soft support for the further dispersion of the guest amine, as if forming a net inside the

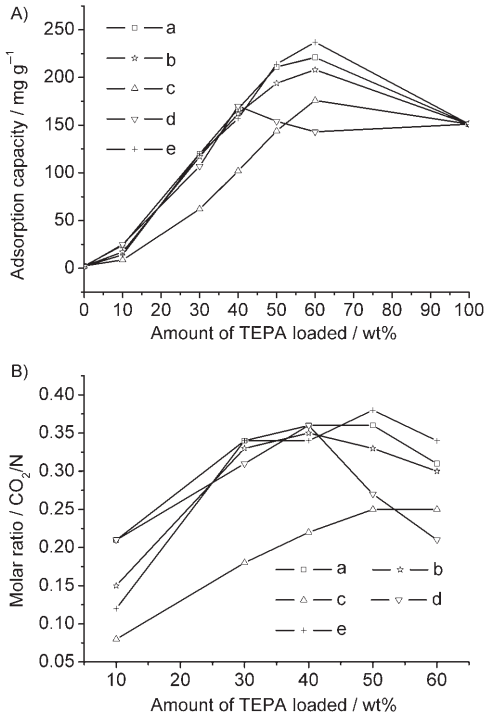

Figure 9. Influence of TEPA on the CO_2 adsorption (A) and CO_2/N molar ratio (B) in MCM-41 samples. a) AM-*n*, b) EM-*n*, c) CM-*n*, d) DM-*n*, and e) PM-*n*. CO_2/N molar ratio: the molar ratio of adsorbed CO_2 to the amine groups in the composites.

pore to divide the tiny space within the channel into infinitesimal ones. Hence, the loaded amine can be dispersed more subtly on these micelles, which not only improves the dispersion of the amine, but also elevates the capture efficiency of CO_2 by the composite, because the collision probability between the target CO_2 molecules in the gas stream and the adsorptive sites in the channel of the adsorbent is enhanced. Without the assistance of template micelles in the channel, CM-*n* samples have a lower capability than AM-*n* in the capture of CO_2 as expected. In fact the CM-*n* sample has another disadvantage in comparison with AM-*n*, which is the cost. One gram of CM contains one gram of mesoporous silica, but one gram of AM consists of only about half a gram of silica because of the existence of the template micelles occluded in the channel. As shown in Table 3, one gram of silica supports two grams of TEPA in the AM-50 sample. However, one gram of silica only supports one gram of TEPA in the CM-50 sample, which is half of that in the AM-50 sample. Hence, the cost can be cut in half by using AM to replace CM as the support. The lower cost plus the higher efficiency in dispersion of amine enables the as-synthesized mesoporous silica to be more competitive than the template-free analogue in the preparation of new CO_2 capturers.[21]

Effect of template state on CO_2 adsorption by the MCM-41 composite: To investigate further the impact of the CTAB template in the amine-containing composite on the adsorption of CO_2, a special support named MT was prepared by impregnating the template-free MCM-41 sample (CM) with 50 wt% CTAB for comparison with sample AM. Both AM and MT samples contain the same amount of CTAB, about 50 wt%, but in the former the CTAB is in the original template micelles occluded in the channel of MCM-41, whereas in the latter the CTAB is incorporated in the calcined MCM-41 sample through impregnation. In other words, the CTAB in the AM sample is inherently dispersed within the channel of MCM-41, while in the MT sample the CTAB is added to the MCM-41 through a postsynthesis procedure. It is very likely that the dispersion and distribution of CTAB in the two samples are different more or less; therefore, the effect of the distribution state of CTAB in MCM-41 on the final adsorption capability of CO_2 can be assessed through comparison of AM and MT along with the corresponding composites.

Table 3. TEPA, silica, and template contents per 100 grams of composite.

Sample	AM-50	DM-50	CM-50	MT-50
template [g]	25	23	0	25
silica [g]	25	27	50	25
TEPA [g]	50	50	50	50
kind of template	CTAB	DTAB	–	CTAB

CTAB alone does not possess any capacity in the adsorption of CO_2 and its profile of CO_2 TPD is linear (not shown). The composite of MT-50, fabricated through impregnation of 50 wt% TEPA on the MT support, exhibits a CO_2 adsorption capacity (155 mg g^{-1}) much lower than that of AM-50 (211 mg g^{-1}), despite the former having the same amount of CTAB and TEPA as the latter. This difference indicates the strong influence of the distribution of CTAB in MCM-41 on the CO_2 capture. In the AM sample, CTAB surfactant disperses in the pore like spokes in a wheel with the cation head rooted on the silica wall through electrostatic interaction, and thus the TEPA guest can be dispersed in the space between the "spokes". In the MT sample, however, CTAB congregates in the pore of MCM-41 in a tangled manner. Therefore, the distribution of amine in MT is not as good as that in AM, which leads to lower accessibility of the amine so that the efficiency of the guest in the adsorption of CO_2 is relatively low, resulting in a smaller adsorption capacity in the MT-50 sample.

To understand the synergy of the cationic surfactant with TEPA in the adsorption of CO_2, three other samples of mesoporous silica (EM, PM, and DM) occluded with different kinds or amounts of surfactant are utilized as carrier to support the amine. As elucidated in Figure 9A, three series of composites prepared from AM, EM, and PM supports (AM-*n*, EM-*n*, and PM-*n*, respectively) possess a similar variation in capturing CO_2 when the loading amount of TEPA increases from 10 to 40 wt%. The observation can be ascribed to the fact that these three supports have a similar spokelike architecture with template occluded in MCM-41. Compared with AM, DM is the as-synthesized MCM-41 prepared with DTAB surfactant whose alkyl chain is shorter

than that of CTAB. So, the mesopore size of the DM sample is smaller than that of AM. This difference between the two supports will affect the incorporation and distribution of amine guests.

At the same loading amount of 10 wt%, the samples of AM-10, DM-10, and CM-10 present CO_2 adsorption capacities of 24, 25, and 8.8 mg g^{-1}, respectively. The obvious difference among these values originates from the different distribution of TEPA in the porous supports. When TEPA is encapsulated in AM, it distributes in the palisade of the CTAB micelle, perhaps enveloping or interacting with the micelles to give better accessibility to the CO_2 molecules, similar to that reported in SBA-15[21] and as shown schematically in Figure 10, although the available data do not allow a detailed discussion of the mechanism involved. In the DM support, the TEPA distribution is similar to that in AM, except for the kind of template, as DTAB is the template occluded in the channel instead of CTAB. In the case of CM, however, the guest TEPA primarily enters the pores of the support where TEPA conglomerates in the silica pores. Referring to Figure 10, it is clear that the dispersion of the amine guest in the palisade of the micelle (such as that in AM) is better than that in the pores of CM, because the TEPA can be anchored on the micelles to avoid conglomeration.[21] Consequently, AM-10 and DM-10 have a larger adsorption capacity and higher CO_2/N (the adsorbed CO_2 to the amine groups) molar ratio than the CM analogues (Figure 9B).

When the loading of TEPA rises to 50 wt%, there are different variations in the adsorption capacity of these composites. For the samples derived from AM, EM, and PM supports, their adsorption capacities increase slowly after TEPA loading over 50 wt%. However, DM-50 exhibits a lower CO_2 adsorption capacity (154 mg g^{-1}) than that of DM-40 (170 mg g^{-1}), and the adsorption capability of DM-60 (143 mg g^{-1}) further declines. Referring to the molar ratio of adsorbed CO_2 to amine groups as shown in Figure 9B, it is assumed that there is an optimal loading amount of TEPA dispersed in the MCM-41 support occluded with the template micelle, depending on the type and number of micelles reserved in the channel of the support. As for the DM support, the optimal loading amount of TEPA is 40 wt% and the theoretical maximum number of TEPA molecules needed to be supported on each DTAB molecule is about 1.84 (Table 2). When the loading amount of TEPA reaches 50 wt%, the redundant TEPA may coat the external surface of the sample and hinder the diffusion of CO_2 into the pores, resulting in a relatively low CO_2 adsorption capacity (154 mg g^{-1}). The DM-60 sample becomes viscous, mirroring the coverage of the external surface by the amine, and its CO_2 adsorption capacity further declines to 143 mg g^{-1}.

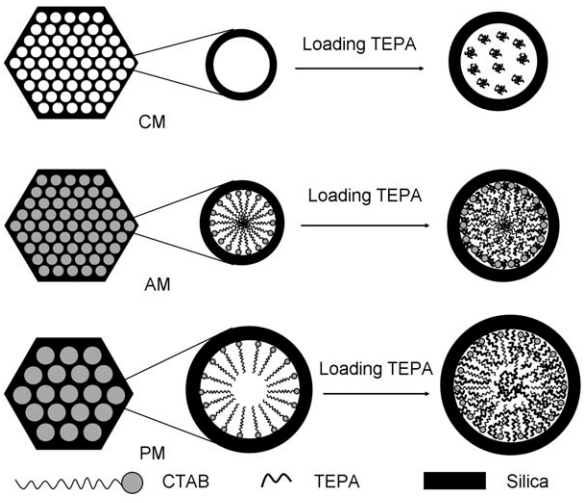

Figure 10. Schematic diagram depicting the influence of the template occluded in a channel of MCM-41 on the distribution of TEPA.

CTAB possesses a carbon chain longer than that in DTAB; hence, the average diameter of the CTAB micelle is bigger than that of the DTAB micelle. Consequently, more TEPA molecules can be dispersed in the palisade of the CTAB micelle. When the loading of TEPA further increases to 50 wt%, the CO_2 adsorption capacity of the AM-50 sample rises to 211 mg g^{-1}. As the loading amount of TEPA further increases to 60 wt%, the resulting AM-60 composites possess an enhanced CO_2 adsorption capacity of 221 mg g^{-1}.

However, the CO_2/N molar ratio of the adsorbent, which mirrors the average efficiency of capturing CO_2 by the amine group located in the composite, decreases from 0.36 (AM-50) to 0.33 (AM-60). Therefore, combining the CO_2/N molar ratio with the CO_2 adsorption capacity of the composite, the optimal loading amount of TEPA on the AM support is determined to be 50 wt%, in which every CTAB molecule can anchor about three TEPA molecules (Table 2). It is more interesting that the theoretically optimal ratio of TEPA molecules supported by DTAB to that by CTAB is 0.58 (1.84/3.18 = 0.58), which closes to the square of the ratio of carbon-chain lengths, $(12/16)^2 = 0.56$. As mentioned before, the longest carbon chain of the surfactant determines the radius of the micelle formed by the surfactant, governing the sectional area of the micelle and impacting the optimal loading amount of the amine guest.

On the basis of these results, it is safe to infer that amine can be distributed much better in the palisade of the as-synthesized mesoporous silica than in the pores of the template-free analogue.[21] Nonetheless, whether amine is dispersed in the palisade or in the pores of the support, the resulting adsorption capacity for CO_2 is always higher than that of the amine alone. To capture the target molecule CO_2 in a gas stream, it is necessary for the amine to be spread on a support to contact the adsorbate, and thus the dispersion state seems crucial for the amine to exert its adsorption function. The AM sample provides a suitable geometric microenvironment for the dispersion and distribution of amine; those amines anchored on micelles can avoid conglomeration and form an efficient web within the channel, elevating both the number of adsorptive sites and the accessibility of amine in the adsorption of CO_2. In addition, the AM sample has two advantages when used as a support:

1) a simpler synthesis procedure which omits the calcination process and saves energy and time; and 2) the lower cost, because it has larger loading amounts of amine and higher CO_2 adsorptive capacity.

Cycle adsorption of CO_2 by the amine–MCM-41 composite: For practical use, the adsorbent should not only possess a high adsorptive capacity for pure CO_2, but also display a stable cyclic adsorption–desorption performance in dilute CO_2 during prolonged operation. Figure 11 illustrates the adsorptive capacities of the AM-50 sample under cyclical adsorption–desorption of CO_2 performed using pure CO_2 and a 1:19 (v/v) CO_2/N_2 mixture. The sample exhibits a high adsorption capacity at low CO_2 concentrations, and the value achieved in 5% CO_2 (200 mg g^{-1}) is close to that in pure CO_2 (211 mg g^{-1}). It should be pointed out that the adsorption capacity in the sixth adsorption cycle at 5% CO_2 concentration remains 183 mg g^{-1}, which is still higher than the known values reported in the literature.[18,19,21] The high adsorption capacities of the composite, especially at low concentrations of CO_2, during prolonged cyclic operation suggest that the sample may be useful for practical applications.

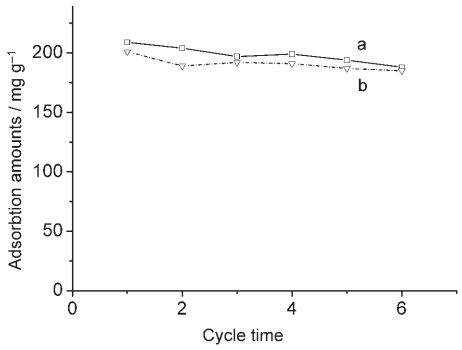

Figure 11. Cyclical adsorption of CO_2 by AM-50 in a) pure CO_2 and b) CO_2/N_2 (1:19, v/v) mixture.

Conclusion

The template micelle reserved in the as-synthesized MCM-41 sample can be used to support/anchor TEPA for preparing efficient CO_2 capturers. The amount, the type, and the distribution of the surfactant occluded in the channel of the support have strong influences on the final CO_2 adsorption capacity of the resulting composites. With the spokelike structure of the micelle in the channel, as-synthesized MCM-41 (AM) is the most competitive candidate for the preparation of efficient CO_2 capturers, as it not only saves the energy and time need to remove the template and reduces the production of pollutants, but also enhances the effectiveness of encapsulated amine for CO_2 adsorption. With the same loading amounts of amine, the composite based on the AM occluded with CTAB possesses a CO_2 adsorption capacity much higher than that derived from common template-free MCM-41 (CM). Moreover, the composite with AM as the host can save about half of the expensive mesoporous silica in the CO_2 capturer, which is crucial to decreasing the cost of CO_2 adsorption.

Experimental Section

Material synthesis: Fabrication of MCM-41 was performed according to the literature.[36] Silica aerosol (3 g) was added to NaOH solution (0.5 M, 45 mL) under stirring and heating to dissolve the additive, then a solution (25 mL) containing CTAB (4.5 g) was added dropwise with stirring at room temperature. The pH value of the solution was adjusted to 11.5 using HCl solution (2 M). After stirring continuously for an additional 6 h, the gel mixture was heated statically at 100 °C for 72 h. Mesoporous materials were recovered by filtration, washed with distilled water, and air-dried to give the sample named AM. For comparison, part of the AM sample was calcined at 550 °C for 6 h in air to remove the template, or extracted with ethanol at 30 °C for 2 h to partially remove the template, giving the samples denoted as CM or EM, respectively. In addition, an MCM-41 sample with different pore size was prepared using DTAB as template. The obtained sample was also air-dried and denoted as DM. Pore-enlarged MCM-41 was synthesized using TMB as swelling agent with a TMB/CTAB ratio of 4.[24] The sample obtained, without calcination, was extracted using ethanol at 30 °C for 2 h to remove TMB and denoted as PM. For comparison with AM, a sample termed MT was prepared by impregnating CTAB at 50 wt % into the CM sample and the resulting material was used as a support. The weight percentage of template and silica in the support were measured by thermogravimetric analysis (TGA).

TEPA was incorporated in MCM-41 through impregnation. The given amount of TEPA was dissolved in ethanol (10 g) under stirring for 0.5 h, and then MCM-41 support (0.2 g) was added. After stirring and refluxing for 2 h, the mixture was evaporated at 80 °C followed by drying at 100 °C for 1 h. These composites were denoted as Support-*n*, where *n* represents the weight percentage of amine in the composite. For example, when AM was used as the support and loaded with 60 wt % TEPA, the obtained sample was named AM-60, which contained 40 wt % AM support and 60 wt % TEPA.

Methods: The composites were characterized by powder XRD, recorded on an ARL XTRA diffractometer using $Cu_{K\alpha}$ radiation (power 40 kV, 20 mA) in the 2θ range from 0.5 to 8°. TGA was carried out in an airflow from 35 to 600 °C with a heating rate of 10 °C min^{-1}. Infrared tests were performed on a Bruker Vedtor22 instrument combined with the conventional KBr wafer technique. Nitrogen adsorption isotherms at −196 °C were measured on a Micromeritics ASAP 2020 volumetric adsorption analyzer, and the sample was outgassed for 2 h in the degas port of the apparatus at 50 °C before measurement.[21] Elemental analysis was performed on Heraeus CHN-O-Rapid instrument (Germany).

To check whether the TEPA was inclined to penetrate into the hydrophobic palisade layer of the micelle, several supports were utilized to load the amine to examine the impact of the structure of the support on the morphology of the resulting amine-containing composite. These supports include quartz, AM, and the calcined MCM-41 (CM). Three zeolites, NaA, KA, and NaY, with pore sizes of 0.4, 0.3, and 0.74 nm and surface areas of 800, 740, and 766 m^2 g^{-1}, respectively,[37] were also employed. All the samples were prepared through wet impregnation with the TEPA-to-support weight ratio of 1:1. TEPA was dissolved in ethanol under stirring for 0.5 h, and then the support was added. After stirring for 2 h, the mixture was evaporated at 80 °C followed by drying at 100 °C for 1 h.

Adsorption: CO_2 adsorption by the solid adsorbent was performed in the manner reported previously.[21] In a typical process, sample (75 mg) with a mesh size of 20–40 was placed in a U-type quartz reactor with an inner diameter of 4 mm and a length of 350 mm, heated in a flow of N_2 (99.995%) at a rate of 8 °C min^{-1} to 100 °C, and kept at 100 °C for 2 h. Prior to the adsorption of CO_2 (99.999%) at a given temperature, a

blank TPD run was carried out to confirm that no desorption occurred. Subsequently, a fixed amount of CO_2 (pure or different CO_2 concentrations diluted with N_2) was injected at the given temperature. When the adsorption finished, the sample was purged with a helium flow for at least 2 h, and then the CO_2 TPD was performed at a rate of 2.5 °C min^{-1} to 100 °C.[15] The liberated CO_2 was detected by an "online" Varian 3380 gas chromatograph and quantitatively measured by the external standard method. In the cyclic adsorption–desorption tests, the sample was allowed to readsorb CO_2 as soon as the entire desorption process at 100 °C was finished. A Netzsch STA449C TG/DSC-MS analyzer was also employed to monitor the adsorption and desorption of CO_2 on the AM-50 sample using helium as the carrier gas, in a manner similar to that reported in the literature.[14,21] In a typical CO_2 adsorption experiment, the sample (20 mg) was preheated under a helium flow (30 mL min^{-1}) at 100 °C for 2 h and then cooled to 75 °C, followed by the introduction of CO_2 (5% in helium) into the system at a flow rate of 30 mL min^{-1}. Meanwhile, the increase in the weight of the sample was recorded. For the desorption of CO_2, the sample that had adsorbed CO_2 at a given temperature was purged with a helium flow at 35 °C for 1 h, and was then heated to 100 °C at a rate of 2.5 °C min^{-1}, followed by holding the sample at 100 °C for 0.5 h. The desorption effluent was simultaneously analyzed by MS. In addition, a blank run was carried out with an empty crucible on the TG balance before it was used for samples, and calibrations for gas composition changes were made to account for differences in buoyancy.

Acknowledgements

Financial support from NHTRDP973 (2007CB613301), the NSF of China (20773601, 20673053, and 20373024), 863 projects of the Chinese Science Committee, and the Analysis Center of Nanjing University is gratefully acknowledged.

[1] J. M. Melillo, A. D. Mcguire, D. W. Kicklighter, B. Moore, C. J. Vorosmarty, A. L. Schloss, *Nature* **1993**, *363*, 234–240.
[2] I. Omae, *Catal. Today* **2006**, *115*, 33–52.
[3] C. S. Song, *Catal. Today* **2006**, *115*, 2–32.
[4] E. Rinker, S. S. Ashour, O. C. Sandall, *Ind. Eng. Chem. Res.* **2000**, *39*, 4346–4356.
[5] R. V. Siriwardane, M. S. Shen, E. P. Fisher, *Energy Fuels* **2003**, *17*, 571–576.
[6] N. D. Hutson, *Chem. Mater.* **2004**, *16*, 4135–4143.
[7] O. Leal, C. Bolívar, C. Ovalles, J. J. Carcía, Y. Espidel, *Inorg. Chim. Acta* **1995**, *240*, 183–189.
[8] M. L. Gray, Y. Soong, K. J. Champagne, J. Baltrus, R. W. Stevens, P. Toochinda, S. S. C. Chuang, *Sep. Purif. Technol.* **2004**, *35*, 31–36.
[9] H. Yoshitake, T. Yokoi, T. Tatsumi, *Chem. Mater.* **2002**, *14*, 4603–4610.
[10] H. Yoshitake, T. Yokoi, T. Tatsumi, *Chem. Lett.* **2002**, 586–587.
[11] T. Yokoi, H. Yoshitake, T. Tatsumi, *J. Mater. Chem.* **2004**, *14*, 951–957.
[12] T. Yokoi, H. Yoshitake, T. Tatsumi, *Chem. Mater.* **2003**, *15*, 4536–4538.
[13] P. J. E. Harlick, A. Sayari, *Ind. Eng. Chem. Res.* **2006**, *45*, 3248–3255.
[14] H. Y. Huang, R. T. Yang, D. Chinn, C. L. Munson, *Ind. Eng. Chem. Res.* **2003**, *42*, 2427–2433.
[15] N. Hiyoshi, D. K. Yogo, T. Yashima, *Chem. Lett.* **2004**, *33*, 510–511.
[16] S. Kim, J. Ida, V. V. Guliants, Y. S. Lin, *J. Phys. Chem. B* **2005**, *109*, 6287–6293.
[17] R. A. Khatri, S. S. C. Chuang, Y. Soong, M. Gray, *Ind. Eng. Chem. Res.* **2005**, *44*, 3702–3708.
[18] X. Xu, C. Song, J. M. Andresen, B. G. Miller, A. W. Scaroni, *Energy Fuels* **2002**, *16*, 1463–1469.
[19] X. Xu, C. Song, J. M. Andresen, B. G. Miller, A. W. Scaroni, *Microporous Mesoporous Mater.* **2003**, *62*, 29–45.
[20] R. S. Franchi, P. J. E. Harlick, A. Sayari, *Ind. Eng. Chem. Res.* **2005**, *44*, 8007–8013.
[21] M. B. Yue, Y. Chun, Y. Cao, X. Dong, J. H. Zhu, *Adv. Funct. Mater.* **2006**, *16*, 1717–1722.
[22] R. Ryoo, C. H. Ko, M. Kruk, V. Antochshuk, M. Jaroniec, *J. Phys. Chem. B* **2000**, *104*, 11465–11471.
[23] A. Sayari, M. Kruk, M. Jaroniec, I. L. Moudrakovski, *Adv. Mater.* **1998**, *10*, 1376–1379.
[24] M. F. Ottaviani, A. Moscatelli, D. Desplantier-Giscard, F. D. Renzo, P. J. Kooyman, B. Alonso, A. Galarneau, *J. Phys. Chem. B* **2004**, *108*, 12123–12129.
[25] A. Sayari, *Angew. Chem.* **2000**, *112*, 3042–3044; *Angew. Chem. Int. Ed.* **2000**, *39*, 2920–2922.
[26] R. Denoyel, E. S. Rey, *Langmuir* **1998**, *14*, 7321–7323.
[27] H. Zhao, K. L. Nagy, J. S. Waples, G. F. Vance, *Environ. Sci. Technol.* **2000**, *34*, 4822–4827.
[28] B. Marler, U. Oberhagemann, S. Vortmann, H. Gies, *Microporous Mater.* **1996**, *6*, 375–383.
[29] W. Hammond, E. Prouzet, S. D. Mahanti, T. J. Pinnavaia, *Microporous Mesoporous Mater.* **1999**, *27*, 19–25.
[30] J. Sauer, F. Marlow, F. Schüth, *Phys. Chem. Chem. Phys.* **2001**, *3*, 5579–5584.
[31] H. Kunieda, K. Ozawa, K.-L. Huang, *J. Phys. Chem. B* **1998**, *102*, 831–838.
[32] P. Agren, M. Lindén, J. B. Rosenholm, J. Blanchard, F. Schüth, H. Amenitsch, *Langmuir* **2000**, *16*, 8809–8813.
[33] R. Zana, *Adv. Colloid Interface Sci.* **1995**, *57*, 1–64.
[34] W. D. Harkin, *Physical Chemistry of Surface Films*, Reinhold, New York, **1952**, Chapter 4.
[35] F. Kleitz, W. Schmidt, F. Schüth, *Microporous Mesoporous Mater.* **2003**, *65*, 1–29.
[36] S. C. Shen, X. Chen, S. Kawi, *Langmuir* **2004**, *20*, 9130–9137.
[37] C. F. Zhou, Y. Cao, T. T. Zhuang, W. Huang, J. H. Zhu, *J. Phys. Chem. C* **2007**, *111*, 4347–4357.

Received: September 15, 2007
Published online: February 18, 2008

